

The Equilibrium Structure and Hydrodynamical Evolution of Non-Self-Annihilating-Light Dark Matter-Admixed White Dwarfs

Chan Ho Sang

Department of Physics, The Chinese University of Hong Kong, Shatin, Hong Kong.

(Dated: November 16, 2021)

The equilibrium structure (ES) and hydrodynamics evolution of non-self-annihilating light dark matter admixed white dwarfs (DMAWD) are still open questions in the field of astrophysics. In this paper, the static spherically symmetrical ES of DMAWD had been studied. We studied the effects of these DM on the ES of DMAWD by investigating the mass, radius, ratio of DM to normal matter (NM) radii and ratio of DM to NM masses versus DM and NM central density. The presence of DM tends to decrease the allowed mass and radius of NM. We identify three kinds of ES: 1. The NM and DM having comparable masses and radii. 2. A small size DM halo surrounding an NM core. 3. NM mass smaller than normal white dwarfs. We also found that accretion of DM is capable of squeezing NM towards neutron drip. We study the hydrodynamics evolution of the DMAWD by using the W.E.N.O hydrodynamics code. We choose to study the first kind of ES, and the results show that it is stable under perturbation. We found that comoving and counter moving oscillation modes, found for dark matter admixed neutron stars, also exist for DMAWD. However, this paper still consist of research gap and limitations.

I. INTRODUCTION

A. Background Information And Motivation

Technological advancement made it possible for physicists to observe and analyze distant astronomical objects. In particular, the rotational velocity of galaxy as a function of distance from their center had been well studied. For example, Rubin and Ford in the 1970s[1] found an asymptotically flat rotating velocity at large distance from the galactic center. The rotational velocity determined from doppler shift can be extended well beyond the visible region of a galaxy[1]. The results suggest that most of the matter in the universe consist of the so called dark matter (DM) which are different than the normal matter (NM) that we know. The structure and properties of DM were unknown to physicists. The standard cosmological model suggested that at the very early universe, cold DM perturbation had grown when the temperature fell below MeV range and hence structures of DM formed[1]. We do expect that there should be considerable DM in the interstellar medium. It is possible that stars or compact stars could accrete DM particles into their interior. Hence we expect that DM should exist in some stars and compact stars. One of our goals is to study how the presences of DM could alter the equilibrium structure (ES) of stars and compact stars.

To be specific, DM can be classified as self-annihilating or non-self-annihilating[7]. In this paper, we shall regard non-self-annihilating DM as DM only, while stating self-annihilating DM using its full name. Effects of self-annihilating DM on main-sequence evolution has been studied by Leung, S-C., et-al.[5] Freese, Katherine, et-al.[13]. On the other hand, effects of DM on compact stars such as white dwarfs and neutron stars also attract wide interests in the field of astrophysics. In particular,

ES of spherically symmetric white dwarfs composing of NM and DM particles with mass in the range of $100 \text{ GeV}/c^2$ to $1000 \text{ GeV}/c^2$ has been studied by Wong, K-W., et-al.[6]. ES of white dwarfs composing of NM and DM with particle mass in the range of $1 \text{ GeV}/c^2$ to $100 \text{ GeV}/c^2$ has been studied by Leung, S-C., et-al.[7]. ES of neutron stars composite of NM and DM had been studied by Leung, S-C., et-al.[8][9] and Rezaei, Z. et-al.[10]. While the results from studying white dwarfs show that the presence of DM with particle mass over $10 \text{ GeV}/c^2$ would have only small influence on the ES, DM with mass $1 \text{ GeV}/c^2$ would produce a DM core of $0.1M_\odot$ and affects the Chandrasekhar limit and global structure of the white dwarf[7]. Despite NM and DM having comparable radii and masses for neutron stars, results also show that neutron stars containing DM with particle mass $1 \text{ GeV}/c^2$ would produce a neutron star core of a few kilometers radius surrounded by a ten-kilo-meters sized DM halo[8][10]. Similar studies have not been studied for white dwarfs. We would like to see whether these effect would be found on DM admixed white dwarfs (DMAWD). Effects of DM with smaller particle mass to the ES of DMAWD are subjects of future exploration.

While the popular candidates of DM, such as neutralino, Inert Higgs doublets, etc. would have particle masses at least GeV/c^2 scale or above[2], it is possible for DM particle to have mass below GeV/c^2 scale. We define DM having mass below GeV/c^2 scale as light DM. There have been increasing interest in light DM in recent years. The XENON10 collaboration shows possibility of DM in the range $20 \text{ MeV}/c^2$ to $1 \text{ GeV}/c^2$ [3]. Direct search detectors also shows possibility of DM with mass below $500 \text{ MeV}/c^2$ [4]. Previous studies by Leung, S-C., et-al. show that decreasing DM particle mass tends to create larger effects on ES of DMAWD[7]. Nevertheless, the baryonic mass of NM component of a white dwarf

has mass in MeV/c^2 scale, and so we expect that DM with particle mass smaller than GeV/c^2 range would have considerable effects on the ES of DMAWD. It would therefore be an interesting question how light DM would affect the ES of a DMAWD.

We study the spherically symmetric ES of DMAWD having range of DM mass from $0.1 \text{ GeV}/c^2$ to $0.3 \text{ GeV}/c^2$ in $0.1 \text{ GeV}/c^2$ steps. The individual mass, radius, ratio of DM to NM radii and ratio of DM to NM masses versus the central densities of the two components will be studied. In our model, the light DM is assumed to be an ideal completely degenerate Fermi gas. We choose this as an extension of the previous studies by Leung, S-C., et-al. who study Fermionic spin $\frac{1}{2}$ DM in GeV/c^2 mass range. Moreover, the ES of DMAWD would be under the joint effect of DM and NM central densities, but their explicit dependences were not studied in any previous literature. While the previous works were based on the general relativistic formalism using the TOV equation, we note that the General Relativity (GR) parameters of white dwarfs are typically 10^{-4} [11]. Therefore, it would be safe to assume newtonian gravity in constructing the ES. However, as we will show, in some extreme cases, the GR parameter of some ES could reach level of neutron stars, for which general relativistic effects become important. In most cases, it is still safe to use newtonian approximation.

We are also interested in the hydrodynamics evolution of DMAWD. The Weighted Essentially Non-Oscillatory (W.E.N.O) hydrodynamics code developed by Wong, K-W., et-al.[6] provide an excellent tool to simulate the hydrodynamics evolution of DMAWD. We noted that, previous results by Wong, K-W., et-al. only focus on the hydrodynamics evolution of DMAWD with a small DM core. The hydrodynamics evolution of DMAWD that have comparable DM and NM radii and masses, if they exist, is still unknown. Previous studies show that there are DM driven and NM drive mode[7]. But studies on radial oscillation of dark matter admixed neutron stars by Leung, S-C., et-al.[9] show that it is possible to have a co-moving and counter-moving mode between NM and DM when they are having comparable masses and radii. We would like to see whether similar results hold for DMAWD.

II. METHODOLOGY

A. The DMAWD Model Construction

As mentioned in the introduction, the spherically symmetric ES will be constructed assuming newtonian gravity. In the hydrostatic equilibrium case, the Euler equation will be reduced to

$$\frac{dP_1(r)}{dr} = -\frac{\rho_1(r)G}{r^2}(M_1(r) + M_2(r)), \quad (1)$$

$$\frac{dP_2(r)}{dr} = -\frac{\rho_2(r)G}{r^2}(M_1(r) + M_2(r)). \quad (2)$$

From now on we label DM (NM) quantities with sub-script 1(2). Quantities without subscript refer to both NM and DM. P is the pressure, ρ is the density and $M(r)$ is the total mass enclosed at a radial distance r .

The differential equation for $M(r)$ under spherical symmetry consideration will then be

$$\frac{dM_1(r)}{dr} = 4\pi r^2 \rho_1, \quad (3)$$

$$\frac{dM_2(r)}{dr} = 4\pi r^2 \rho_2. \quad (4)$$

While both the NM and DM are assumed to be ideal completely degenerate Fermi gas, the pressure P of the ideal Fermi gas could be expressed in terms of a dimensionless quantity x as follows [11]:

$$P = \frac{m^4 c^5}{\hbar^3} \phi(x), \quad (5)$$

$$\frac{\rho Y_e}{m_B} = \frac{m^3 c^3 x^3}{3\pi^2 \hbar^3}. \quad (6)$$

Here c is the speed of light, \hbar is the reduced Planck constant, m is the degenerate particle mass. Y_e is the mean number of degenerate particles per parent particle. m_B is the mass of the parent particle. The pressure function can be expressed as[11]

$$\phi(x) = \frac{x(1+x^2)^{\frac{1}{2}}(\frac{2x^2}{3} - 1) + \ln[x + (1+x^2)^{\frac{1}{2}}]}{8\pi^2}. \quad (7)$$

Now for typical white dwarfs, $Y_{e2} \approx 0.5$, $m_2 = 0.511 \text{ MeV}/c^2$, $m_{B2} \approx 931 \text{ MeV}/c^2$. [11] For DM, $m_{B1} = m_1$ and $Y_{e1} = 1$ since DM exists alone without any parent particle.

We want to solve Eqs. 1 - 4 for the hydrostatic equilibrium configuration. We follow the idea by Jackson et-al.[14] with extension to the 2 fluid case. It is natural to make use of the dimensionless variable x and rewrite the pressure gradient

$$\frac{dP}{dr} = \frac{dP}{dx} \frac{dx}{dr}. \quad (8)$$

$$(9)$$

Now noted that

$$\frac{dP}{dx} = \frac{m^4 c^5}{3\pi^2 \hbar^3} \frac{x^4}{\sqrt{1+x^2}}, \quad (10)$$

$$\frac{Y_e}{m_B} \frac{d\rho}{dr} = \frac{m^3 c^3 x^2}{\pi^2} \frac{dx}{dr}. \quad (11)$$

One can rewrite the pressure gradient

$$\frac{dP}{dr} = \frac{Y_e m c^2}{3m_B \hbar^3} \frac{x^2}{\sqrt{1+x^2}} \frac{dx}{dr}. \quad (12)$$

Now we are equipped to rewrite (1),(2),(3),(4) into

$$\frac{dx_1}{dr} = -\frac{m_{B1} G}{Y_{e1} m_1 c^2} \frac{\sqrt{1+x_1^2}}{r^2 x_1} (M_1 + M_2), \quad (13)$$

$$\frac{dM_1}{dr} = \frac{4m_1^3 c^3 m_{B1}}{3\pi \hbar^3 Y_{e1}} x_1^3 r^2, \quad (14)$$

$$\frac{dx_2}{dr} = -\frac{m_{B2} G}{Y_{e2} m_2 c^2} \frac{\sqrt{1+x_2^2}}{r^2 x_2} (M_1 + M_2), \quad (15)$$

$$\frac{dM_2}{dr} = \frac{4m_2^3 c^3 m_{B2}}{3\pi \hbar^3 Y_{e2}} x_2^3 r^2. \quad (16)$$

To eliminate the constants, we can further introduce dimensionless quantities \bar{M} and \bar{r} such that $M = M_0 \bar{M}$ and $r = R_0 \bar{r}$. Now we choose M_0 and R_0 such that

$$R_0 = \sqrt{\frac{3\pi \hbar^3}{Gc}} \frac{Y_{e1}}{2m_1 m_{B1}}, \quad (17)$$

$$M_0 = \sqrt{\frac{3\pi \hbar^3}{Gc}} \frac{Y_{e1} c^2}{2Gm_{B1}^2}. \quad (18)$$

Then we can rewrite Eqs. 13-16 in dimensionless form:

$$\frac{dx_1}{d\bar{r}} = -\frac{\sqrt{1+x_1^2}}{\bar{r}^2 x_1} (\bar{M}_1 + \bar{M}_2), \quad (19)$$

$$\frac{d\bar{M}_1}{d\bar{r}} = x_1^3 \bar{r}^2, \quad (20)$$

$$\frac{dx_2}{d\bar{r}} = -\frac{Y_{e1} m_1 m_{B2}}{Y_{e2} m_2 m_{B1}} \frac{\sqrt{1+x_2^2}}{\bar{r}^2 x_2} (\bar{M}_1 + \bar{M}_2), \quad (21)$$

$$\frac{d\bar{M}_2}{d\bar{r}} = \frac{m_2^3 m_{B2} Y_{e1}}{m_1^3 m_{B1} Y_{e2}} x_2^3 \bar{r}^2. \quad (22)$$

This 4 sets of differential equations will be used to compute the density profile of DMAWD. The numerical computational scheme will be presented in the next section.

B. The Computational Scheme And The Choice Of Central Density

In general, the differential equation would need to be solved numerically. We would adopt the RK4 computational scheme to obtain high accuracy. We define the

first grid to be the center of the DMWAD. Now for given central densities for DM and NM $\rho_1[0]$ and $\rho_2[0]$, we can compute $x_1[0]$ and $x_2[0]$ using Eq. 6. We would iterate x_1 and x_2 until the atmospheric density is reached. The atmospheric density is set to prevent the differential equation from entering the unstable region when x is too small. Typically, we would set the atmospheric density to be 10^{-5} times the central density. Once the atmospheric density is reached, the mass of the fluid component will be frozen. The masses and radii R of NM and DM are taken to be the values of M and R at the grid point where the atmospheric density is reached. The step size is set to be $\frac{1}{100}$.

We choose the central densities of both NM and DM ranging from 10^9 kgm^{-3} to 10^{14} kgm^{-3} . The upper bound is set to prevent the NM reaching neutron drip density where the completely degenerate Fermi gas equation of state is no longer so accurate. The lower bound is set so that both NM and DM component are degenerate. The justification is the follow. For typical white dwarfs, their mass had lower limit of $0.5M_\odot$ which corresponds to a central density of 10^9 kgm^{-3} [16]. The degenerate effect of electrons happen when the electron matter wavelength λ is comparable to the average separation $\frac{V}{N}$ between electron. Where V is the volume and N is the number of electrons.

$$\lambda^3 \approx \frac{V}{N}. \quad (23)$$

And hence, by relating average separation with density, we have

$$\lambda^3 \approx \frac{Y_{e1} \rho_1}{m_{B1}}. \quad (24)$$

We expect the same argument hold for Fermionic DM particle. Thus we obtain the relation of DM central density for DM to be degenerate

$$\frac{Y_{e1} \rho_1}{m_{B1}} \approx \frac{Y_{e2} \rho_2}{m_{B2}}. \quad (25)$$

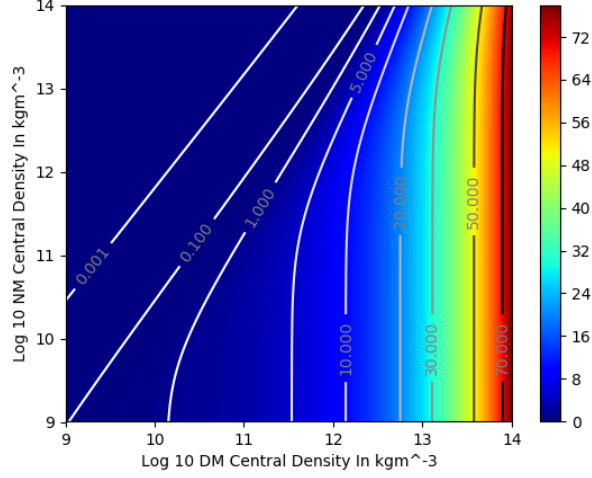
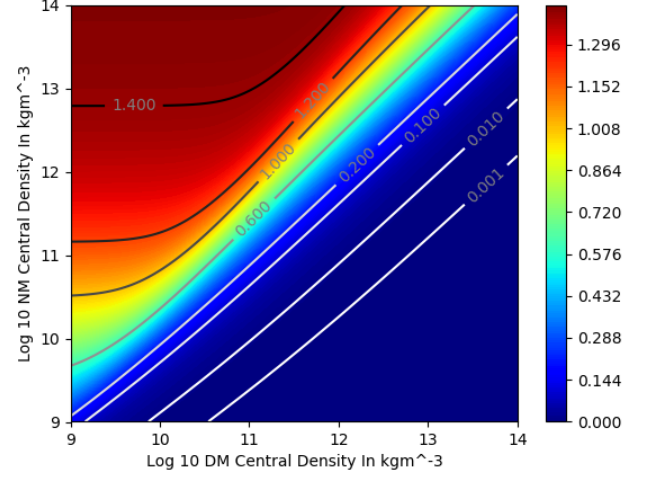
We thus obtain

$$\rho_1 \approx 10^9. \quad (26)$$

This justify our choice of range of central density of NM and DM.

C. The W.E.N.O Hydrodynamics Code

After solving for the ES of DMAWD, we would identify and choose suitable ES. Their hydrodynamics evolution will be simulated using W.E.N.O hydrodynamics code

DM Mass In Solar Mass Contour Plot For DM Particle Mass $0.1\text{GeV}/c^2$ FIG. 1. DM mass versus DM and NM central density contour plot for DM particle mass $0.1\text{ GeV}/c^2$.NM Mass In Solar Mass Contour Plot For DM Particle Mass $0.1\text{GeV}/c^2$ FIG. 2. NM mass versus DM and NM central density contour plot for DM particle mass $0.1\text{ GeV}/c^2$.

developed by Wong, K-W., et-al. We would study the time evolution of the following quantities for both NM and DM under radial velocity perturbation: 1. Central densities. 2. Densities at half radii of the static DMAWD (half radius density). 3. Radii. We would analyze the results by using discrete Fourier transform to find out the corresponding oscillation frequency and match the oscillation mode.

III. RESULTS ANALYSIS AND DISCUSSION

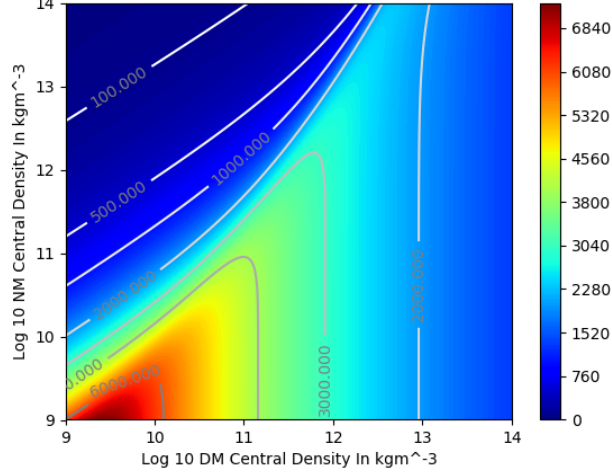
A. The ES Of DMAWD

1. Mass Versus Density Contour Plots

Generally, the dependence of NM and DM masses on the NM and MD central densities are similar for these three set of DM particle mass. We included their contour plots for DM particle mass $0.1\text{ GeV}/c^2$ as FIG.1, FIG.2 for reference. NM mass contour plot and DM mass contour plot are nearly symmetric about the contour line 0 for masses ratio and radii ratio contour plots (see FIG.5 and FIG.6). Whenever NM (DM) central density is much larger than DM (NM) central density, the mass contour plot become NM (DM) dominating and the NM (DM) mass versus NM and DM central densities relations correctly reduced to that of single component fluid limit. The maximum NM mass is around $1.4M_\odot$ (solar mass) which agrees with the Chandrasekar mass of a normal white dwarf. The maximum mass for DM changes significantly as the DM particle mass increase. It is consistent with the fact that, self-gravitating degenerate particle would have smaller maximum mass as the particle mass increases[7][8]. We would like to

point out that, the ES that consist of extraordinary DM maximum mass $70M_\odot$ for DM particle mass $0.1\text{ GeV}/c^2$ lies on region where DM central density is near 10^{14} kgm^{-3} . However, as shown in the appendix, these region would have GR parameter around 10^{-1} where newtonian gravity is no longer so accurate. Hence whether these extraordinary DM masses would be not so accurate results due to newtonian approximation, will needed to be confirmed by solving the relativistic TOV equation.

The NM and DM masses is in general under mutual effect of NM or DM central densities changes. NM (DM) mass is insensitive to DM (NM) central density changes only when NM (DM) is dominating. These region is presented by horizontal (vertical) contour lines for NM (DM) mass contour plot. These region increase (decrease) for NM (DM) mass contour plot when DM particle mass increase, which means the effect of NM (DM) to their NM (DM) mass become more (less) significant in our chosen central density range, so that NM (DM) become more (less) dominating. For fixed NM (DM) central density, when the DM (NM) central density gradually increase, there exists region where increasing DM (NM) central density would results in a significant decrease in NM (DM) mass. They are presented as contours line that are closely packed and located on area of significant color changes. As the DM particle mass increase, the closely packed contour lines for NM (DM) mass contour plot, gradually move towards high (low) DM (NM) central density region. The closely packed contour lines are denser and are having larger slope. We can see that the presence of DM tends to decrease the mass of NM for fixed central density. For example, the maximum mass of NM when it is having NM central density 10^{14} kgm^{-3} could reduced to $0.2M_\odot$. It is consistent with the findings from Leung, S-C., et-al.[7] In other words, the presence

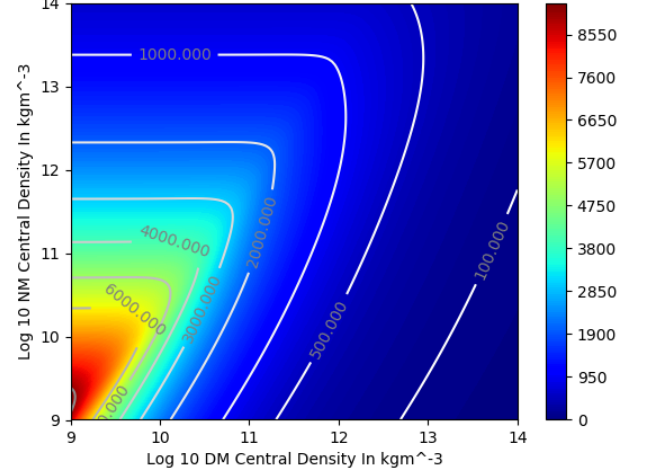
DM Radius In km Contour Plot For DM Particle Mass $0.1 \text{ GeV}/c^2$ FIG. 3. DM radius (in km) versus DM and NM central density contour plot for DM particle mass $0.1 \text{ GeV}/c^2$

of DM could squeeze NM with smaller mass into sufficiently high density so that they could be described as degenerate Fermi gas. As DM particle mass increase, to significantly squeeze small NM mass, the DM central density must be much higher than that of NM.

2. Radius Versus Density Contour Plots

Generally, the dependence of NM and DM radii on the NM and DM central densities are similar for these three set of DM particle masses. We included their contour plots for DM particle mass $0.1 \text{ GeV}/c^2$ as FIG.3 and FIG.4 for reference. NM radius contour plot and DM radius contour plot are nearly symmetric about the contour line 0 for masses ratio and radii ratio contour plot (see FIG.5 and FIG.6). We found that NM (DM) radius is insensitive to DM (NM) central density changes when DM (NM) is dominating, which are represented by horizontal (vertical) contours line. In that case the NM (DM) radius versus central density relations correctly reduced to that of single component fluid limit. These region increase (decrease) when DM particle mass increase. Which means the effect of NM (DM) to NM (DM) radius become more (less) significant in our chosen central density range, and that NM (DM) become more (less) dominating. Similar to mass contour plot, there is a region where NM (DM) radius is very sensitive to DM (NM) central density changes. They are presented by the closely packed contour lines located on significant color changes. As the mass of DM particle increase, these contour line become more closely packed and move towards high (low) DM (NM) central density region.

Combining the results from mass contour plot, we find that in general, the presence of DM tends to decrease

NM Radius In km Contour Plot For DM Particle Mass $0.1 \text{ GeV}/c^2$ FIG. 4. NM radius (in km) versus DM and NM central density contour plot for DM particle mass $0.1 \text{ GeV}/c^2$

the radius and increase the central density of NM. Take the contour plot of NM mass for example, to conserve NM mass, the ES of DMAWD should lies on constant NM mass contour line. When the admixed DM mass (and hence DM central density) is small, the NM radius is not sensitive to DM central density changes. NM remained having the nearly same central density and radius. But as DM mass gradually increase, the ES would goes along the densely packed NM mass contour lines, in that case there would be a significant increment in central density and decrement in radius. This feature could be understood as the DM particle providing extra gravitational pull to squeeze the whole DMAWD. This feature allows DMAWD composing NM that would have mass smaller than normal white dwarfs. The presence of DM could squeeze such less massive NM into density that is high enough to be degenerate. The radius of such DMAWD depends on how much DM is in the DMAWD. If the DM mass is not large enough to squeeze the NM, the NM could extend in radial direction with their radius larger than a normal white dwarf. We have computed some of such ES and comparing their NM masses and radii with that of a typical $1M_{\odot}$ white dwarf having the same central density in TABLE.1. These DMAWD could be possibly formed when DM was accreted by less massive stars such as brown dwarfs, which are not supposed to be massive enough to be a white dwarf. However, as DM particle mass increase, NM will become dominating in masses and radii contour plot, and DM can squeeze less massive NM into high density only if DM had high central density. Therefore it would be less likely to have such ES in that case.

	NM Mass	DM Mass	NM Radius
Normal White Dwarf	$1 M_{\odot}$	-	5500 km
DMAWD $0.2 \text{ GeV}/c^2$	$0.86 M_{\odot}$	$0.02 M_{\odot}$	5700 km
DMAWD $0.3 \text{ GeV}/c^2$	$0.58 M_{\odot}$	$0.05 M_{\odot}$	6700 km
DMAWD $0.3 \text{ GeV}/c^2$	$0.48 M_{\odot}$	$0.06 M_{\odot}$	7000 km
DMAWD $0.3 \text{ GeV}/c^2$	$0.19 M_{\odot}$	$0.08 M_{\odot}$	7300 km

TABLE I. Table comparing mass, and NM radius for some ES that are having larger radius and smaller mass when compared to a $1M_{\odot}$ white dwarf, they are having same NM central density but different DM particle mass. Here, M_{\odot} represent solar mass.

Log 10 Radius Ratio Of DM To NM For DM Particle Mass $0.1\text{GeV}/c^2$

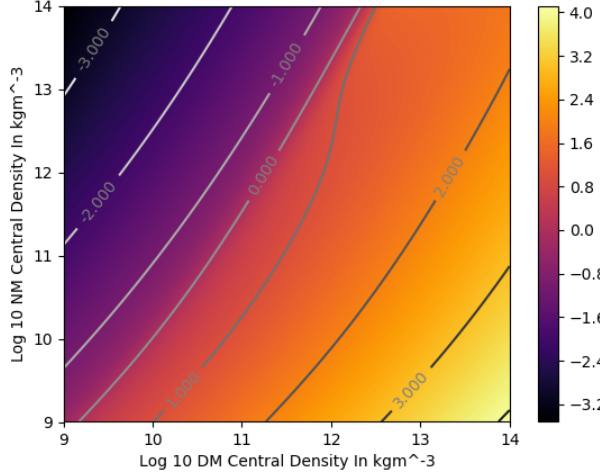


FIG. 5. Log 10 of DM to NM radii ratio contour plot for DM particle mass $0.1 \text{ GeV}/c^2$

3. Radii Ratio And Masses Ratio Versus Density Contour Plots

We have computed the ratio of DM to NM radii and DM to NM masses. We included their contour plot for DM particle mass $0.1 \text{ GeV}/c^2$ as FIG.5 and FIG.6 for references. We adopted the log10 scale to reflect whether NM and DM would have comparable radii or comparable masses. The contour line 0 reflects that NM and DM having comparable radii or they would have comparable masses. The general behaviour of the DM to NM radii and DM to NM masses ratio is similar for these 3 sets of DM particle mass. Region where DM (NM) is more massive than NM (DN) would have ES that DM (NM) surrounding an NM (DM) core. The contour line 0 for DM to NM radii ratio do not exactly but almost coincide with that of DM to NM masses ratio. We see that a new class of ES where DM and NM having comparable masses and radii. One of the typical density profile had been included as FIG.7 for reference. As DM particle mass increase, the contour line 0 for DM to NM masses ratio and DM to NM radii ratio shift together towards right. It

Log 10 Mass Ratio Of DM To NM For DM Particle Mass $0.1\text{GeV}/c^2$

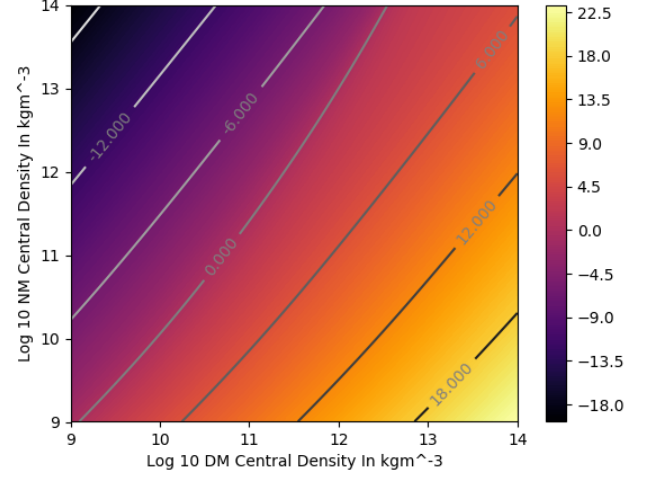


FIG. 6. Log 10 of DM to NM masses ratio contour plot for DM particle mass $0.1 \text{ GeV}/c^2$

means that it is more unlikely to have DMAWD having comparable radii and comparable masses or a relatively massive DM halo surrounding NM core. In that case, NM become dominating and these ES exist only when DM central density is higher than the NM central density.

We also noticed that, the 0 contour lines nearly coincide with the closely packed contour lines for mass and radius contour plots. Hence, the 0 contour lines may mark the onset of DM or NM domination on DMAWD. Near the 0 contour line, the competition between NM and DM is the most, hence at that region, ES such as DMWAD having comparable NM and DM masses and radii could exist. They are the results of such competition between NM and DM. For even larger DM particle mass, these contour lines will shift towards right and hence in our chosen central density range, the DMAWD will be NM dominating. This is consistent with the shifting of the closely packed contour lines, and the increase (decrease) of NM (DM) dominating region for mass and radius contour plot. DM would have considerable effect to NM only when DM central density is much higher than NM central density. This can be understood as DM particle mass increase, the density required for it to be degenerate would be much higher, hence in our chosen density range, the DM is not so degenerate and the effect of degenerate Fermi gas will be mainly come from NM.

When DM win over the domination, DM is capable to squeeze the NM into its interior core. Combining the results from radius and mass contour plot, these small DMAWD with DM surrounding a less massive NM core. This new class of ES is an extended founding with the that from Leung, S-C., et-al., who show that new class of ES of dark matter admixed neutron stars having

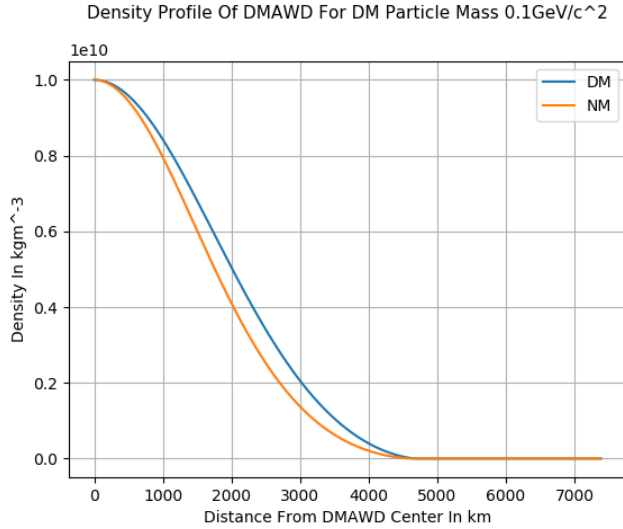


FIG. 7. Density profile for a typical DMAWD having comparable DM and NM masses and radii

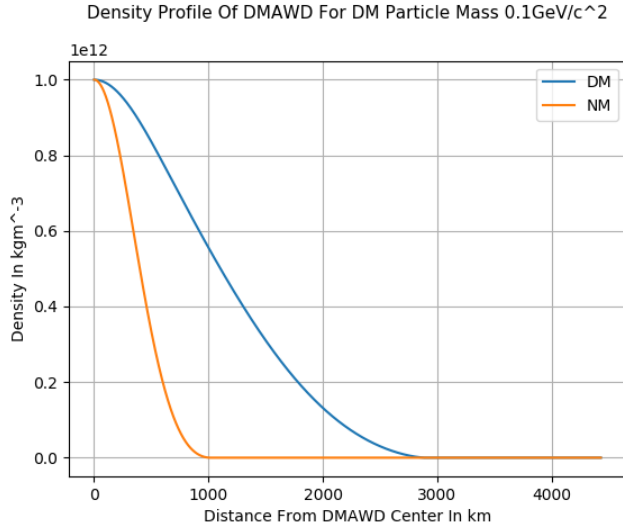


FIG. 8. Density profile for a typical DMAWD with massive DM halo surrounding NM core

extremely small NM core and DM halo[8]. We show that it is also possible for DMAWD. A typical density profile had been included as FIG.8 for reference. To get a sense of how small such DMAWD could be, note that Mars is having radius approximately 3400 km, while Pluto is having radius approximately 1100 km, and Earth is having radius approximately 6300 km[15].

4. DM Accretion Of NM Towards Neutron Drip

Previously, we have show that the increase in DM mass can significantly increase the central density of NM

by considering the closely packed contour lines of mass and radius contour plot. We found that for larger DM particle, the contour line attains larger slope. And the increment of DM mass required for significant DM central density changes become smaller. Take DM particle $0.3 \text{ GeV}/c^2$ as an example, to squeeze NM with mass $1M_{\odot}$ to neutron drip, the increment in mass is around $0.9M_{\odot}$. Hence for heavier DM particle, only accreting for a small fraction of mass can induce a significant increment of NM central density. The generally accepted model for white dwarfs evolution towards neutron stars is through NM accretion so that white dwarfs could reach its Chandrasaker limit, Type Ia supernova explosion occurs and leave the remaining core to be a neutron star. However, our results show that it is possible to squeeze the DMAWD so that NM central density move towards neutron drip by simply accretion of DM. Whether the results would be a direct evolution to a neutron star, or a Type Ia supernova with smaller white dwarf mass, is still unknown. Although the previous studies show that to accrete considerable DM, the typical time scale exceeds that of cosmic time.[7] However, we see that as DM particle mass increase, it is possible to have an accretion of smaller mass of DM which results in a significant density increment towards neutron drip. To verify this feature, a simulation model that allowed accretion of DM is needed. And unfortunately, this feature is not presenced in the W.E.N.O hydrodynamics code.

B. The Hydrodynamics Evolution Of DMAWD

By using the studies from the previous section, we identify ES consist of comparable DM and NM radius and mass that is not presenced in the previous studies. A typical one is presented in FIG.7 and we would choose this ES to study the hydrodynamics evolution of DMAWD. The mass, radius, escape velocity, GR parameter and free fall time had been included in TABLE.2.

We mainly studied the radial oscillation mode under initial velocity perturbation. We choose the time of simulation to be 5000000 in code unit. This is sufficient when compare with the free fall time of the DMAWD. We choose to implement initial velocity perturbation to both NM and DM using the form

$$v = v_0 \frac{r}{R}. \quad (27)$$

Where R is the radius of either component. We choose v_0 to be $0.0005c$. We would apply initial velocity perturbation for the following three cases

1.Both NM and DM having same initial direction of velocity perturbation of the form (27).

DM Mass	$0.34 M_{\odot}$
NM Mass	$0.25 M_{\odot}$
DM Radius	4700 km
NM Radius	4600 km
free fall time (code unit)	260000
free fall time (second)	1.28
escape velocity	$0.02c$
GR parameter	0.0002

TABLE II. Table summarizing mass, radius, free fall time, escape velocity and GR parameter for the chosen ES for simulating DMAWD hydrodynamics evolution.

2. Only DM having initial velocity perturbation of the form (27).

3. NM and DM having opposite direction of velocity perturbation of the form (27).

While for each case, the central density, half radius density, and radius against time would be studied. The radius is defined as we did in the methodology section.

Our simulation results show that our chosen ES is stable under radial velocity perturbation. For case 1, it can be seen that both NM and DM oscillate periodically and are in phase. We have included the central density oscillation as time for case 1 as FIG.9 for reference. Although NM and DM are having the same initial central density, the maximum central density under time evolution is different. We apply discrete Fourier transform to the central density, half radius density and radius against time datum. The results show that there is a significant peak around frequency 0.2030 Hz which are the same for both DM and NM. It show this DMAWD exist co-moving oscillation mode which is characterized by the frequency 0.2030 Hz. To demonstrate that the two component are co-moving, we have included the momentum profile for DM and NM as FIG.10 and FIG.11 respectively. We see that in different time, NM and DM component are having momentum of the same sign.

For case 2, it can be seen that the oscillating waveform of DM and NM had an relative phase shift. We have included the central density oscillation as FIG.12 for reference. However, they still oscillate in the same direction. We apply Fourier transform to central density, half radius density and radius versus time datum, it show that despite there is a significant peak occurs at frequency 0.2030 Hz, a second maximum occurs at frequency for 0.3248. These two peaks appears for Fourier transform results of half radius density and radius oscillation for both NM and DM. For radius oscillation,

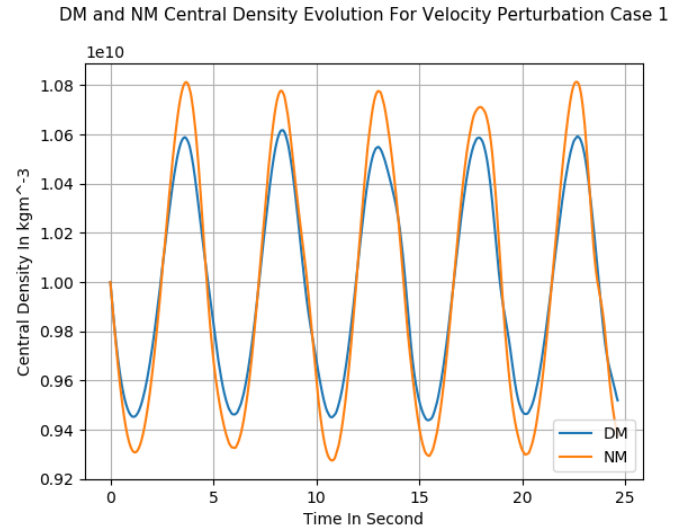


FIG. 9. Central density oscillation as time for our chosen ES in velocity perturbation case 1

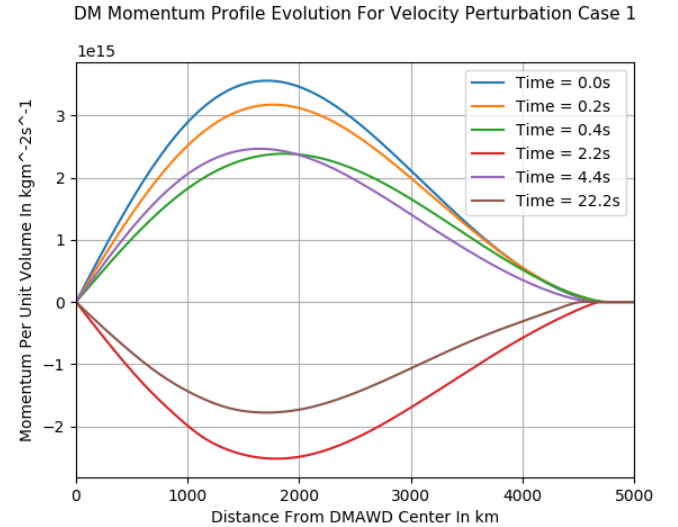


FIG. 10. DM momentum profile at different time for our chosen ES in velocity perturbation case 1

the amplitude of the peak frequency 0.3248Hz exceeds that of 0.2030 Hz. We also include the DM and NM momentum profile evolution as FIG.13 and FIG.14 to demonstrate their motion. We see that DM and NM sometime are co-moving, but sometimes one of the fluid is at rest and the other is not. We believe that some counter-moving mode had been excited in case 2 and become dominating at DMAWD surface.

For case 3, it can be seen the oscillation of DM and NM are out of phase. We have included the central density oscillation as FIG.15 for reference. We apply discrete Fourier transform to central density, half radius density and radius versus time datum. The results show

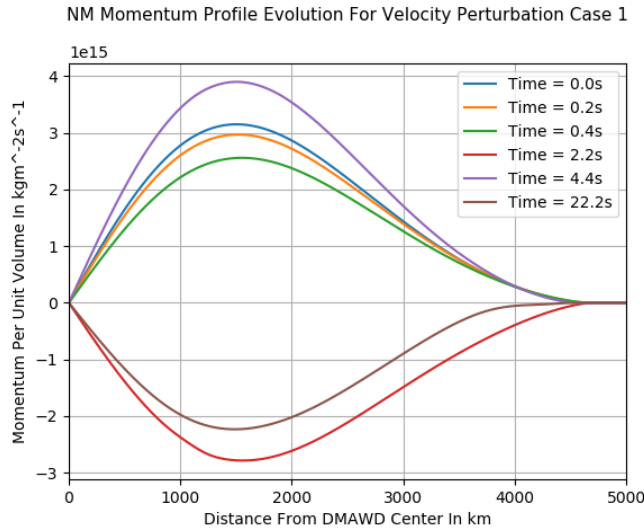


FIG. 11. NM momentum profile at different time for our chosen ES in velocity perturbation case 1

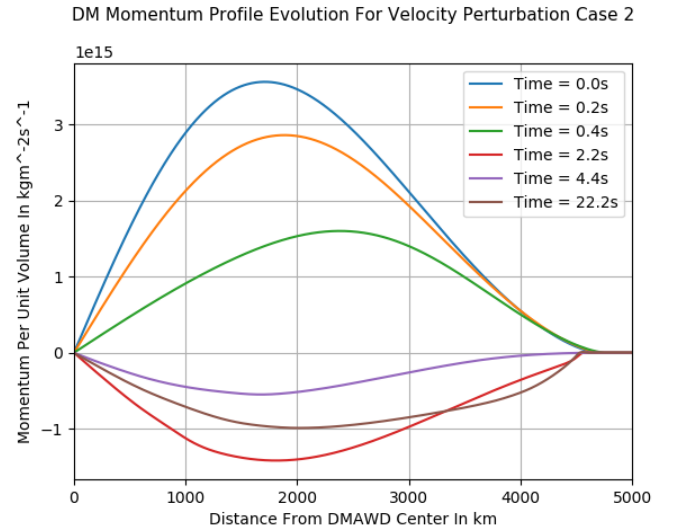


FIG. 13. DM momentum profile at different time for our chosen ES in velocity perturbation case 2

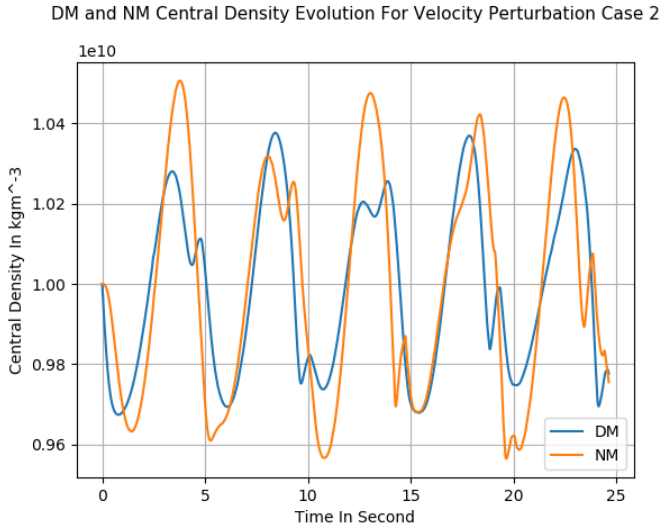


FIG. 12. Central density oscillation as time for our chosen ES in velocity perturbation case 2

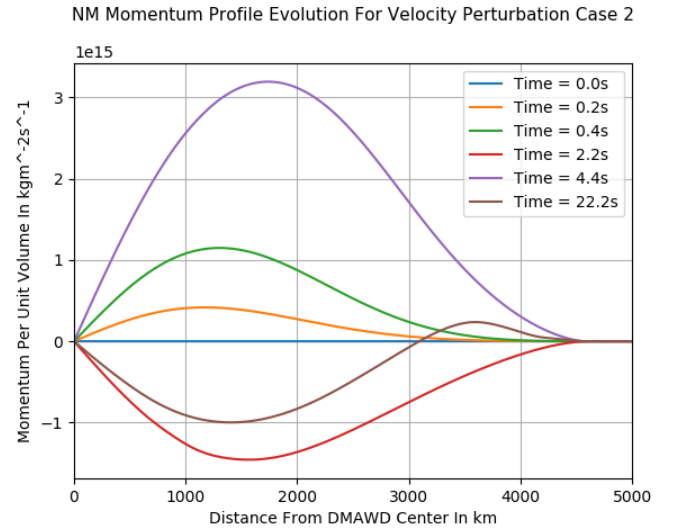


FIG. 14. NM momentum profile at different time for our chosen ES in velocity perturbation case 2

that the peak occurs at frequency 0.3248 Hz. This correspond to the second maximum peak frequency as calculated in case 2. The original peak of 0.2030 Hz become negligible. It show that the dominating frequency had changed from 0.2030 Hz to 0.3248 Hz and the excited oscillation frequency corresponds to 0.3248 Hz. We show that our DMAWD exist counter-moving oscillation mode characterized by the frequency 0.3248 Hz. We see that this frequency exist in case 2, and that DM and NM need not to be exactly out of phase, but they would show a relative phase shift. To demonstrate that they are really counter-moving, the momentum profile at different time for NM and DM had been included as FIG.16 and FIG.17 for reference. We

see that NM and DM are exactly moving in opposite direction for any time.

As shown by previous studies by Leung, S-C., et-al.[9]. There exist oscillation mode for dark matter admixed neutron stars which DM and NM component are co-moving and counter-moving. Although the analysis from Leung, S-C., et-al. focus on neutron stars while using general relativistic formalism to gravity, we see that similar feature can also exist for newtonian DMAWD.

DM and NM Central Density Evolution For Velocity Perturbation Case 3

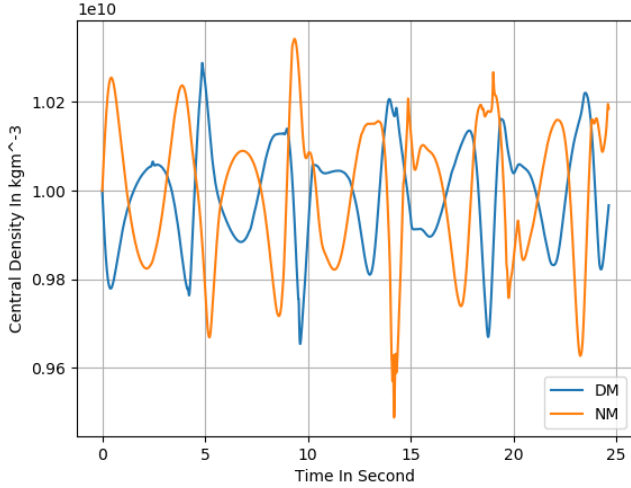


FIG. 15. Central density oscillation as time for our chosen ES in velocity perturbation case 3

NM Momentum Profile Evolution For Velocity Perturbation Case 3

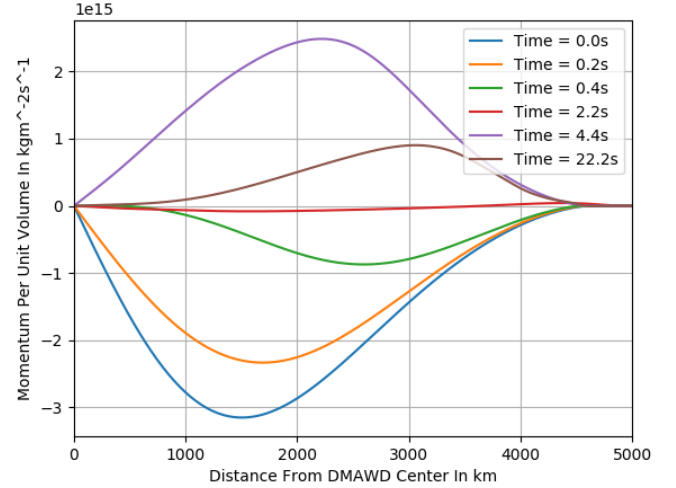


FIG. 17. NM momentum profile at different time for our chosen ES in velocity perturbation case case 3

DM Momentum Profile Evolution For Velocity Perturbation Case 3

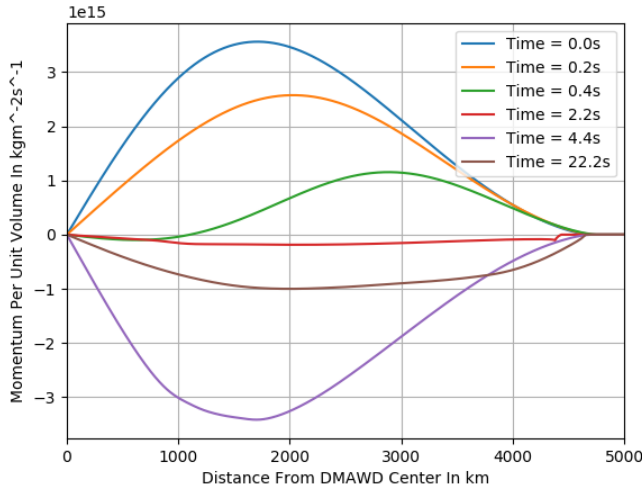


FIG. 16. DM momentum profile at different time for our chosen ES in velocity perturbation case 3

IV. LIMITATION AND FUTURE ASPECT

In constructing the ES of DMAWD, we have adopted the newtonian gravity approximation. However, we noted that at high DM central density range, the GR parameter could reach level of neutron stars and hence our newtonian approximation is not so accurate. We doubt that the extraordinary massive DM halo is the not so accurate results of using newtonian approximation only. To verify whether these massive DM halo really exist, a general relativistic TOV equation is needed for solving the ES of DMAWD.

We have chosen our range of central density from

10^9 kgm^{-3} to 10^{14} kgm^{-3} . However, for lower central density, the DMAWD would be partially degenerate due to the decreasing density of outer part. Hence, the behaviour of NM and DM masses, radii will be different if we consider correction to the equation of state of the outer part of the DMAWD. Moreover, when NM density is over 10^{10} kgm^{-3} , it would become neutron rich and hence the completely degenerate Fermi gas equation of state is no longer so accurate. To have a more realistic model of DMAWD, the neutron equation of state is needed to be considered.

So far we have assumed that the NM and DM are completely degenerate Fermi gas. However, there could be more realistic equation of state for DM.[10] Whether the same feature as predicted from our analysis to ES of DMAWD would still hold if we replace the equation of state of DM, is still unknown. Moreover, finite temperature effect to the equation of state for degenerate Fermi gas is well studied, but in this paper, we had neglected this effect for both studying the ES of DMAWD and the hydrodynamics evolution simulation of DMAWD. To have a more comprehensive study of realistic DMAWD, the equation of state must be carefully chosen.

We claimed that we discover new ES of DMAWD that

1. Having comparable radius and mass
2. A small size DM halo surrounding NM core
3. Having NM mass smaller than normal white dwarfs

Although our simulation results show that one of these chosen ES is stable under perturbation. Whether these ES would be in general, stable, were unknown. We

did not study the stability and fundamental modes of oscillation of the DMAWD in our chosen density range. Therefore, it would be an interesting topic to study whether these new ES of DMAWD would be in general stable.

We claimed to discover it is possible to squeeze NM into neutron drip by simply accreting DM. However, due to the limited feature of W.E.N.O hydrodynamics code, we are unable to simulate DM accretion to DMAWD. In the future, a more comprehensive simulation code should be used to verify what will be the consequence of such DM accretion. Nevertheless, we had studied the hydrodynamics evolution and oscillation mode of DMAWD by investigating only one of the chosen density profile. To have a more comprehensive study on the oscillation mode and stability of general DMAWD, we need a fluid perturbation analysis and 2 sets of eigenvalues problem is needed to solve.

V. CONCLUSION

In this paper, we had studied the ES of DMAWD for DM particle mass $0.1 \text{ GeV}/c^2$ to $0.3 \text{ GeV}/c^2$ in $0.1 \text{ GeV}/c^2$ steps. We identify three kinds of ES: 1.The NM and DM having comparable masses and radii. 2.A small size DM halo surrounding an NM core. 3.NM mass smaller than normal white dwarfs. We also found that accretion of DM is capable of squeezing NM towards neutron drip. The evolution of DMAWD under such DM accretion are still waiting for further exploration.

By using the W.E.N.O hydrodynamics simulation code, we have shown that one of the ES that having comparable NM mass and radius is stable under perturbation. We have identify DM and NM co-moving and counter-moving oscillation mode. We found that the counter-moving mode is specified by an relative phase shift of oscillation between NM and DM and they need not to be exactly moving out of phase. This is an extension findings from previous studies by Leung, S-C., et-al.[9].

However, this paper still consists significant research gap and unanswered question. In general, whether those new class of ES of DMAWD are stable, general relativistic correction to the ES construction of DMAWD and the proper choice of DM equation of state is to be carefully considered.

NM and DM Central Density Fourier Transform For Velocity Perturbation Case 1

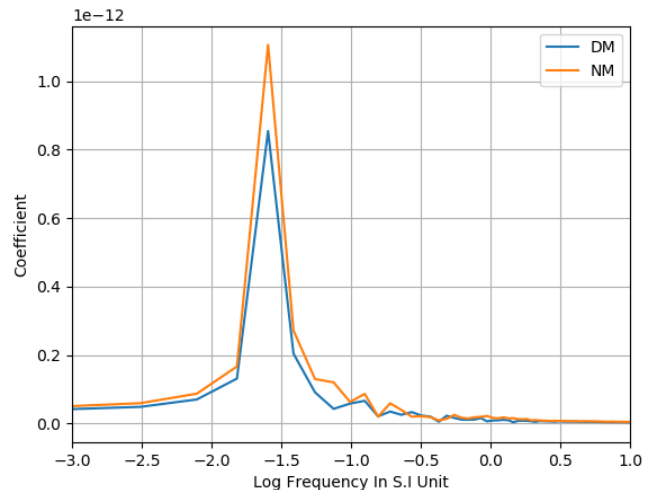


FIG. 18. NM and DM central density oscillation Fourier transform results of velocity perturbation case 1. Noted that DM and NM oscillation shared the same peak

VI. APPENDIX

A. Fourier Transform Results Of DMAWD Hydrodynamics Evolution

We included in this section, some typical Fourier transform results from the hydrodynamics evolution of DMAWD as FIG.18, FIG.19, FIG.20 for reference. Despite including the Fourier transform results of central density oscillation, we also include the Fourier transform results of radius oscillation corresponds to velocity perturbation case 2 to show the counter-moving mode overtaking the co-moving mode.

B. GR Parameter Of DMAWD Construction

To justify our legitimacy of using newtonian approximation to construct our DMAWD, we have computed the GR parameter $\frac{GM_{total}}{R_{max}c^2}$ where R_{max} is the larger radius between NM and DM component. Our results show that in most case the GR parameter is smaller than or equal to order of 10^{-2} so that we are legitimate to use newtonian approximation. The GR parameter contour plots for DM particle mass $0.1 \text{ GeV}/c^2$ had been included as FIG.21 for references. We see that at high DM central density region, the GR parameter could reach order 10^{-1} where newtonian approximation no so accurate and that extraordinary large DM mass ES exist on that region. Hence whether extraordinary large DM mass ES would be a not so accurate results due to newtonian approximation only, would needed to be confirm by considering GR correction.

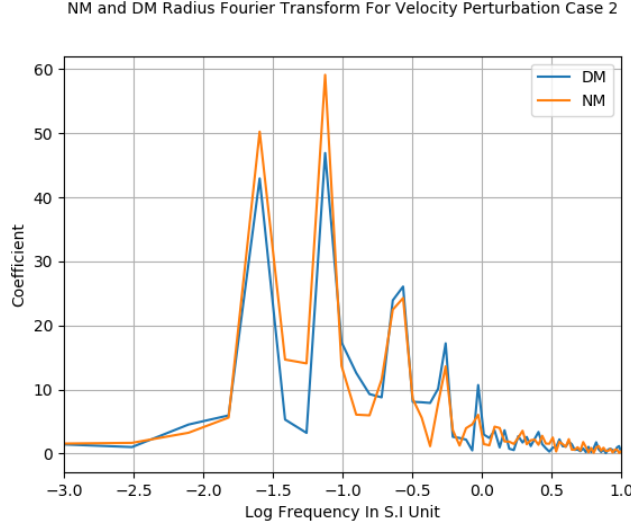


FIG. 19. NM and DM radius oscillation Fourier transform results of velocity perturbation case 2. Noted that the secondary peak overtaking the original peak in case 1

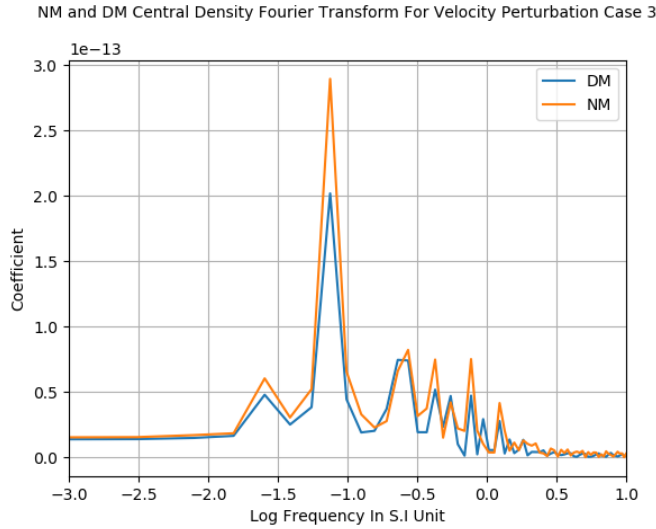


FIG. 20. NM and DM central density oscillation Fourier transform results of velocity perturbation case 3. Noted that the secondary peak completely dominate the oscillation mode

C. Convergence Test For Constructing DMAWD

To test the convergence of our code that construct the ES of DMAWD, we had chosen the ES that had been used to simulate hydrodynamics evolution of DMAWD. We compute the mass of DM and NM, M_1 , M_2 at the 1000th grid from center for reducing step size dh in the code unit by factor of 2, and it had been included in TABLE.3. We see that although we have been adopting RK4 algorithm, the order of accuracy is limited to $O(dh^3)$ due to the choice of initial condition and the implementation of atmospheric density. Nevertheless, the

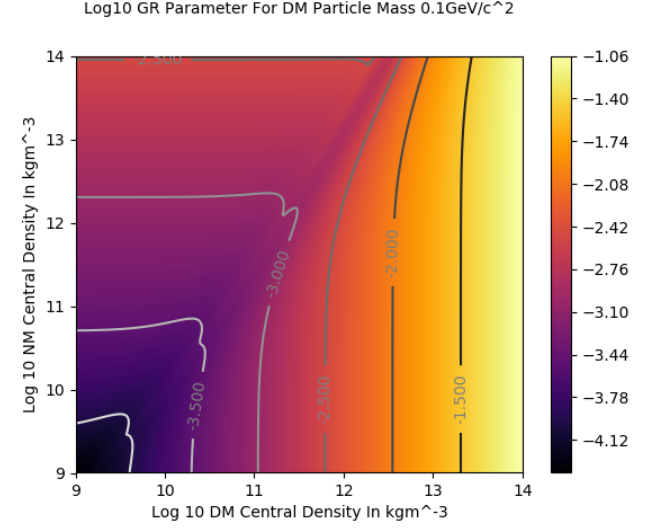


FIG. 21. GR parameter contour plot for DM particle mass $0.1 \text{ GeV}/c^2$.

dh	$\log \frac{M_{1h} - M_{1\frac{h}{2}}}{M_{1\frac{h}{2}} - M_{1\frac{h}{4}}}$	$\log \frac{M_{2h} - M_{2\frac{h}{2}}}{M_{2\frac{h}{2}} - M_{2\frac{h}{4}}}$
0.08	2.998282	2.997686
0.04	2.999570	2.999421
0.02	2.999892	2.999856
0.01	2.999973	2.999964
0.005	2.999993	2.999991
0.0025	2.999999	2.999998

TABLE III. Convergence test for DMAWD construction. The subscript denoted the value of M_1 and M_2 calculated using the corresponding step size

results still converge.

D. Stability Test And Convergence Test Of DMAWD Hydrodynamics Evolution

We have test the stability and convergence of W.E.N.O hydrodynamics code by using the same ES as above. We choose to apply velocity perturbation as case 3. We choose to simulate by using decreasing step size in length and in time dt . The total time is sufficient when compared with free fall time. We have included the evolution of total mass of DM and NM. The result is included as FIG.22 for reference and it show that the simulation converge as we decrease time and length step size. We have calculated the maximum fractional change of total mass, which is at order of 10^{-5} and the result show that the simulation is stable.

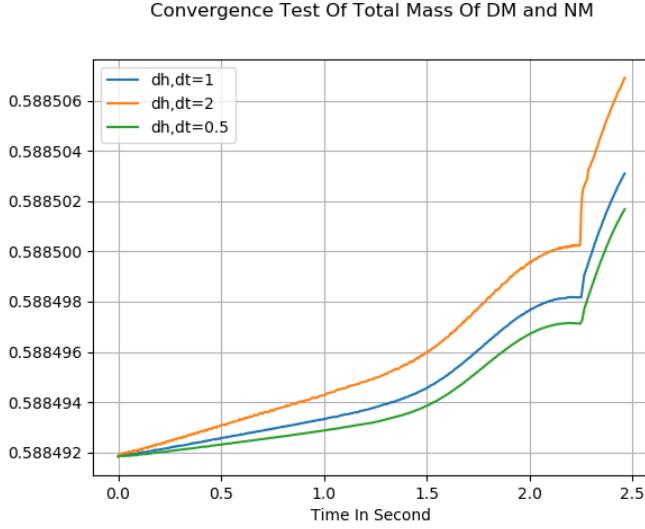


FIG. 22. Convergence and stability test of DMAWD hydrodynamics evolution. The total mass evolution is presented using decreasing step size dh and time step dt

E. References

- [1] Choudhuri, Arnab Rai. "Astrophysics for physicists." Cambridge university press, 2010.
- [2] Bergström, Lars. "Dark matter candidates." New Journal of Physics 11.10 (2009): 105006.
- [3] Essig, Rouven, et-al. "First direct detection limits on sub-GeV dark matter from XENON10." Physical review letters 109.2 (2012): 021301.
- [4] Kouvaris, Chris, and Josef Pradler. "Probing sub-GeV dark matter with conventional detectors." Physical review letters 118.3 (2017): 031803.
- [5] Leung, S-C., "Effects of Non-self-annihilating Dark Matter on Compact Stars and Main-sequence Stars". MA Thesis. The Chinese University of Hong Kong, 2012. Web. 8 Oct. 2018.
- [6] Wong, K-W., "Physical Properties of White Dwarf with a Dark Matter Core". MA Thesis. The Chinese University of Hong Kong, 2011. Web. 8 Oct. 2018.
- [7] Leung, S-C., et-al. "Dark-matter admixed white dwarfs." Physical Review D 87.12 (2013): 123506.
- [8] Leung, S-C., M-C. Chu, and L-M. Lin. "Dark-matter admixed neutron stars." Physical Review D 84.10 (2011): 107301.
- [9] Leung, S-C., M-C. Chu, and L-M. Lin. "Equilibrium structure and radial oscillations of dark matter admixed neutron stars." Physical Review D 85.10 (2012): 103528.
- [10] Rezaei, Z. "Study of Dark-matter Admixed Neutron Stars Using the Equation of State from the Rotational Curves of Galaxies." The Astrophysical Journal 835.1 (2017): 33.
- [11] Shapiro, Stuart L., and Saul A. Teukolsky. Black holes, white dwarfs, and neutron stars: The physics of compact objects. John Wiley Sons, 2008.
- [12] Glendenning, Norman K. Compact stars: Nuclear physics, particle physics and general relativity. Springer Science Business Media, 2012.
- [13] Freese, Katherine, et-al. "Stellar structure of dark stars: A first phase of stellar evolution resulting from dark matter annihilation." The Astrophysical Journal Letters 685.2 (2008): L101.
- [14] Jackson, Chris B., et-al. "Compact objects for everyone: I. White dwarf stars." European journal of physics 26.5 (2005): 695.
- [15] <https://www.nasa.gov/>
- [16] Moroni, PG Prada, and O. Straniero. "C/O white dwarfs of very low mass: 0.33-0.5 M_{\odot} ." Journal of Physics: Conference Series. Vol. 172. No. 1. IOP Publishing, 2009.